

# UC San Diego

## UC San Diego Previously Published Works

### Title

Statistical methodologies for removing the operational effects from the dynamic responses of a high-rise telecommunications tower

### Permalink

<https://escholarship.org/uc/item/1ss4d635>

### Journal

Structural Control and Health Monitoring, 28(4)

### ISSN

1545-2255

### Authors

Ribeiro, Diogo  
Leite, Jorge  
Meixedo, Andreia  
[et al.](#)

### Publication Date

2021-04-01

### DOI

10.1002/stc.2700

Peer reviewed

# Statistical methodologies for removing the operational effects from the dynamic responses of a high-rise telecommunications tower

Diogo Ribeiro<sup>1</sup>  | Jorge Leite<sup>1</sup>  | Andreia Meixedo<sup>2</sup>  | Nuno Pinto<sup>2</sup>  | Rui Calçada<sup>2</sup>  | Michael Todd<sup>3</sup> 

<sup>1</sup>CONSTRUCT-LESE, School of Engineering, Polytechnic Institute of Porto, Porto, Portugal

<sup>2</sup>CONSTRUCT-LESE, Faculty of Engineering, University of Porto, Porto, Portugal

<sup>3</sup>Department of Structural Engineering, University California San Diego, La Jolla, CA, USA

## Correspondence

Diogo Ribeiro, CONSTRUCT-LESE, School of Engineering, Polytechnic Institute of Porto, Porto, Portugal.  
Email: drr@isep.ipp.pt

## Summary

This paper describes statistical methodologies for removing the influence of operational effects from the dynamic responses of a telecommunications tower. The characterization of the dynamic responses of the structure, over a period of 3 months, was based on a continuous monitoring system that included accelerometers, anemometers and a meteorological station. The analysis of the results allowed identifying a significant number of critical events, for which the dynamic response under wind action is significantly amplified, as well as sporadic events, associated with high peak acceleration values, due to the influence of operational effects related to the movement of the lift, technical staff, and equipment. The automatic identification of critical events, based on extreme acceleration values, required the prior removal of operational effects from the records using two distinct methodologies, one based on the principal component analysis (PCA) and the other based on the crest factor (CF) and on autoregressive models (AR). Both methodologies showed efficiency and robustness in eliminating acceleration peaks due to operational effects; however, the methodology based on the CF and AR models proved to be computationally more efficient and resulted on a smaller number of false-positive occurrences in the identification of critical events. The developed methodologies showed potential to be integrated in Structural Health Monitoring (SHM) systems to assess the structural safety and serviceability of telecommunications towers.

## KEYWORDS

autoregressive model, continuous monitoring system, crest factor, operational effects, principal component analysis, telecommunications tower

## 1 | INTRODUCTION

High-rise telecommunications towers are structures in which the dynamic effects induced by wind action can put their operating conditions at risk, mainly due to excessive vibration phenomena. These vibration phenomena generally affect user comfort, health and safety, equipment safety, and the quality of signal transmission.<sup>1,2</sup>

There are numerous cases, some of them recent, of telecommunications towers in which specific phenomena of excessive wind-induced vibration have been reported, for which the dynamic response has been continuously observed with the support of monitoring systems.<sup>1,3,4</sup>

As part of experimental investigations carried out at the Cottbus television tower, in Germany, Beirow and Osterrieder<sup>1</sup> detected events of excessive vibration in the tower by means of several geophones positioned along the concrete shaft, which were associated with vortex-shedding phenomena on the metallic antenna located at the top of the tower. Resonant phenomena were identified under very low temperature conditions ( $-11^{\circ}\text{C}$ ) and prevailing eastward winds, with the maximum accelerations recorded at the top of the antenna in the order of  $3\text{ m/s}^2$ . The study also evaluated the comfort of the technical staff during the resonant vibration events of the tower, which was classified as satisfactory, noting that the location of the technical floors is close to the node of the second vibration mode of the tower, which is mobilized in these circumstances with a frequency equal to 1.2 Hz.

Guo et al.<sup>4</sup> performed vibration measurements on the Guangzhou TV tower, in China, to characterize the dynamic behavior of the structure under extraordinary events, particularly earthquakes and typhoons. Based on the accelerations measured at different locations along the height of the tower during the occurrence of eight typhoons, between August 2008 and July 2011, peak values were recorded between 0.91 mg and 8.35 mg. The tower's performance during the occurrence of typhoons was considered satisfactory, considering a 90% confidence interval in relation to regulatory limits.

Regarding telecommunications towers, the operational effects, related, for example, to neighborhood traffic, lifts, telecommunications equipment, maintenance works, visitors, among others, may significantly affect the assessment of the dynamic responses measured under wind actions, namely, their peak values. Removing the influence of operational effects from the dynamic records is a complex task, especially when their frequency range overlaps or is close to the frequency ranges of the structure and wind actions, invalidating their removal using digital filters.<sup>5</sup> Other environmental effects related to temperature variations, solar radiation, humidity, ice, among others, may influence the dynamic responses of these structures, mainly because the mechanical properties of materials change, sometimes significantly, according to environmental conditions, and may also cause variations in stress state, geometry, and boundary conditions.<sup>5,6</sup>

In the specific field of removing the effects of environmental/operational effects from the dynamic responses of telecommunications towers, no published research has been identified; however, a significant number of studies in the fields of modal identification<sup>7,8</sup> and damage detection<sup>9,10</sup> should be pointed out, in which they are referred to as normalization techniques.

Normalization techniques have been used for the removal of environmental effects, namely temperature, early damage detection, and prevention of false alarms, as changing environmental conditions may impose response variations greater than those induced by damage. Studies on the application of normalization techniques to operational effects are scarce, and the existing ones are mainly related to traffic actions.

Normalization techniques have been applied based on two different approaches<sup>5,6,9-11</sup>: (i) regression-based methods, and (ii) pattern-recognition methods.

The first approach involves the experimental measurement of environmental/operational conditions, together with the dynamic responses, and the establishment of mutual relationships by means of linear regression models, such as multivariate linear regression, and nonlinear regression models, such as nonlinear polynomial or statistical regression.<sup>6</sup> Linear regression models are easy to implement computationally and are widely used to predict the natural frequency values of bridges as a function of temperature.<sup>12,13</sup> Cross et al.<sup>14</sup> points out that nonlinear regression models have better performance in predicting the structural response of bridges as a function of road traffic.

The second approach is based on the application of pattern-recognition methods to measure structural responses in order to identify, and subsequently eliminate, the parts associated with environmental/operational effects. This approach is used in situations where there are no experimental measurements of environmental/operational conditions and is typically more computationally demanding. Moreover, for its efficiency, the variability of the environmental/operational situations that were used in the training/learning phase is particularly important, so that the algorithms can adequately assess their influence on the responses. Among the various available methods, the principal component analysis (PCA),<sup>7,9</sup> the auto-associative neuronal networks (AANN),<sup>15-17</sup> the multilayer perceptron (MLP) neural networks,<sup>18</sup> the factor analysis,<sup>19</sup> the singular value decomposition (SVD),<sup>5</sup> and the Wavelet transforms<sup>10</sup> clearly stand out, as well as other hybrid approaches that result from the combination of some of the previous methods.

The PCA is one of the most widely used methods and is based on the representation of structural responses in the principal component subspace.<sup>20</sup> The principal components are independent from one another and represent distinct contributions to the responses due to actions, eventual damage, noise, among others.<sup>21</sup> Moughty and Casas<sup>6</sup> highlight the simplicity and efficiency of this method in linear problems, where the removal of environmental/operational effects only involves the exclusion of the associated principal components. Based on a numerical model of the Gadiana bridge, Santos et al.<sup>9</sup> simulated the effect of temperature on the structure considering several damage scenarios. From the static displacement records, the authors applied a PCA and concluded that the first five principal components were associated with the global effect of temperature on the structure, while the higher order principal components were associated with induced damage. Still within the scope of this study, the authors tested several criteria to determine the number of principal components to be excluded for removing the temperature effect, with the Broken-Stick criterion showing the best performance. The authors also point out the difficulty of selecting a stable criterion for determining the number of principal components associated with the effects of temperature, which has repercussions on the efficiency and robustness of the PCA method.

Datteo et al.<sup>22</sup> presented the application of a long-term monitoring strategy based on the PCA of autoregressive (AR) parameters, in order to simulate the vibration response of a stand of the Giuseppe Meazza stadium, in Italy. The results showed a good correspondence between the principal components (PCs) and the main environmental conditions (temperature and humidity), in particular, the first PC seemed to be more affected by changing weather conditions, and conversely, the second and third components showed a clearer dependency on operational conditions, such as concerts and football matches.

Thus, this study aims to provide clear and effective contributions regarding some aspects that are presently not sufficiently addressed in the existing bibliography, in particular:

1. Development of computationally efficient methodologies for removing the influence of operational effects on dynamic responses, specifically targeted for operating conditions in telecommunications towers.
2. Demonstrate the importance of removing operational effects in the identification of critical events associated with dynamic amplifications of structural responses under wind actions. In particular, it is intended that the methodologies to be developed minimize the number of false-positives in the detection of such events caused by the influence of operational effects. The success in identifying the number of occurrences, as well as the duration and magnitude of the critical events, is crucial for the evaluation of the operational and safety conditions of the telecommunications tower to be studied.<sup>3</sup>
3. Specifically, for the PCA method, this study aims to define a stable criterion for the removal of the principal components associated with operational effects only. In addition, the acceleration records used for the PCA were derived from the signal division of a single sensor, rather than using information from multiple sensors.

## 2 | MONTE DA VIRGEM TELECOMMUNICATIONS TOWER

The Monte da Virgem telecommunications tower is a transmission tower built in 1995 and located in Vila Nova de Gaia, in northern Portugal. The tower's structure is formed by a 126 m high reinforced concrete shaft and a 51 m high metallic tower, with a total height of 177 m, making it the tallest structure of its kind in Portugal (Figure 1a).

The reinforced concrete shaft has the shape of a hyperboloid, with a hollow circular section and a diameter ranging from 14.3 m, near the base, to 7.7 m, at the top. The diameter of the shaft also varies between 0.40 m, near the base, and 0.30 m, at the top. The shaft has five technical floors consisting of prestressed concrete console slabs (Figure 1c). The floors are located between 94.9 m and 112 m from the base of the shaft, two of them are covered with exterior facades, and the others are exterior with handrails in their outline. Inside the shaft, there is an elevator box and a metallic staircase, supported by metallic beams, interleaved along the height of the shaft and connected to cantilevers fixed to the shaft (Figure 1d).

The metallic mast consists of a spatial lattice formed by three sections along its height, intended for mounting the FM, VHF, and UHF transmission systems, as shown in Figure 1b. The tower has an octagonal base and is fixed to the concrete shaft by means of anchor bolts. The transition from the metallic tower to the shaft is made by means of a concrete slab with a thickness of 1.20 m.

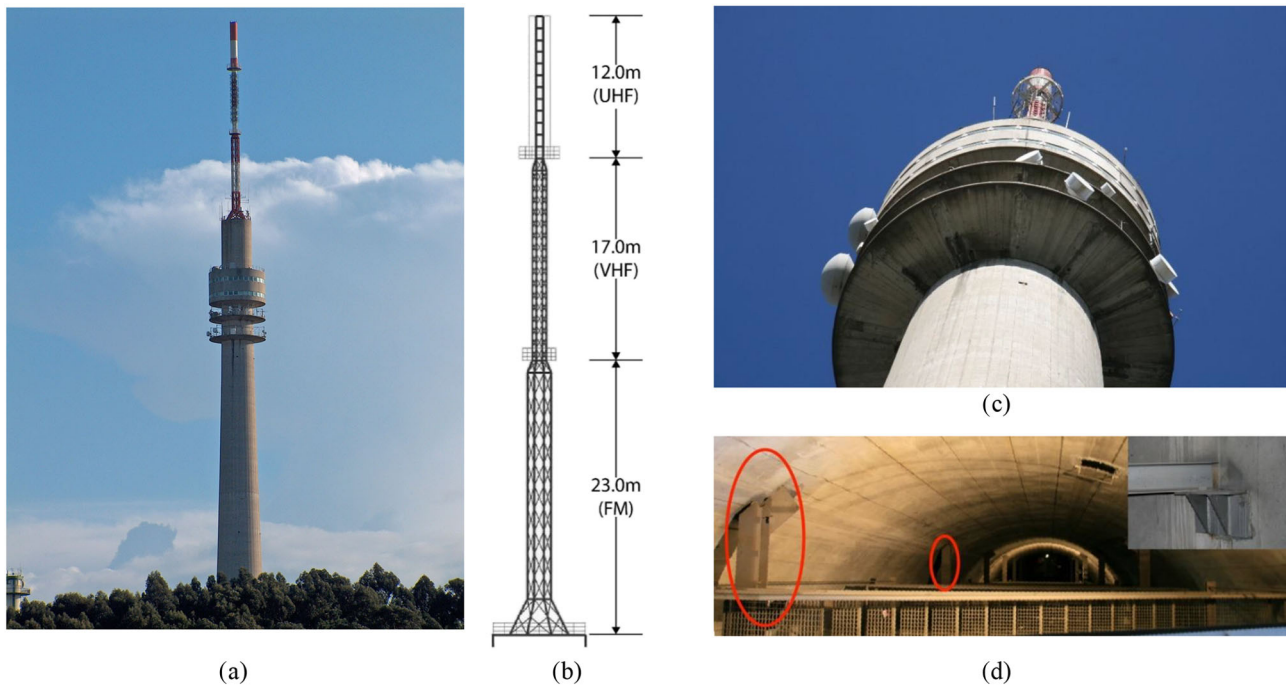


**FIGURE 1** Monte da Virgem telecommunications tower: (a) general view, (b) metallic mast, (c) technical floors, (d) top view of the interior metallic beams and detail of its support on the shaft

### 3 | CONTINUOUS MONITORING SYSTEM

#### 3.1 | Description

The monitoring system installed in the Monte da Virgem tower aims to characterize the maximum accelerations of the structure and the wind regimes.

For this purpose, two piezoelectric accelerometers, PCB model 393B12, two anemometers, VAISALA model WM302, and a PCE-FWS-20 meteorological station were installed in the tower (Figure 2). The accelerometers were positioned at level 104.4 (A1 and A2), directly fixed to the floor, and protected from electromagnetic radiation by means of an aluminum protective case. The accelerations were measured in two radial and orthogonal directions (south–north and west–east), according to the indications of Figure 2, with a sampling frequency equal to 2000 Hz and posteriorly decimated to 50 Hz. The anemometers (An1 and An2) and the meteorological station (Em) were installed on the exterior floor, at level 112.2, in different positions, namely, southwest (SW), northwest (NW), and north (N), and fixed to the sideguard by means of auxiliary structures or directly using metal clamps. The wind speed and direction were instantaneously measured at each 2 s, and no averaging procedure was performed. The limited access to points of the metallic mast located at higher levels was related to safety reasons and also due to electromagnetic interference in the measuring equipment caused by the proximity of the radio signal emitters.

The signal acquisition from the accelerometers and anemometers was performed through a National Instruments cDAQ-9,172 data acquisition system, using analog input modules, NI 9233 and NI 9205, respectively. This system connects to a computer via a USB protocol, which, in turn, is connected to the Web through a router. The meteorological station transmits the data via a wireless protocol to a local receiver, which, in turn, sends the information to the computer through a USB protocol.

#### 3.2 | Results

Based on the analysis of the acceleration's records measured in the structure over a period of 3 months, from September 1 to November 30, 2017, three types of events were identified and designated as noncritical, critical, and sporadic.

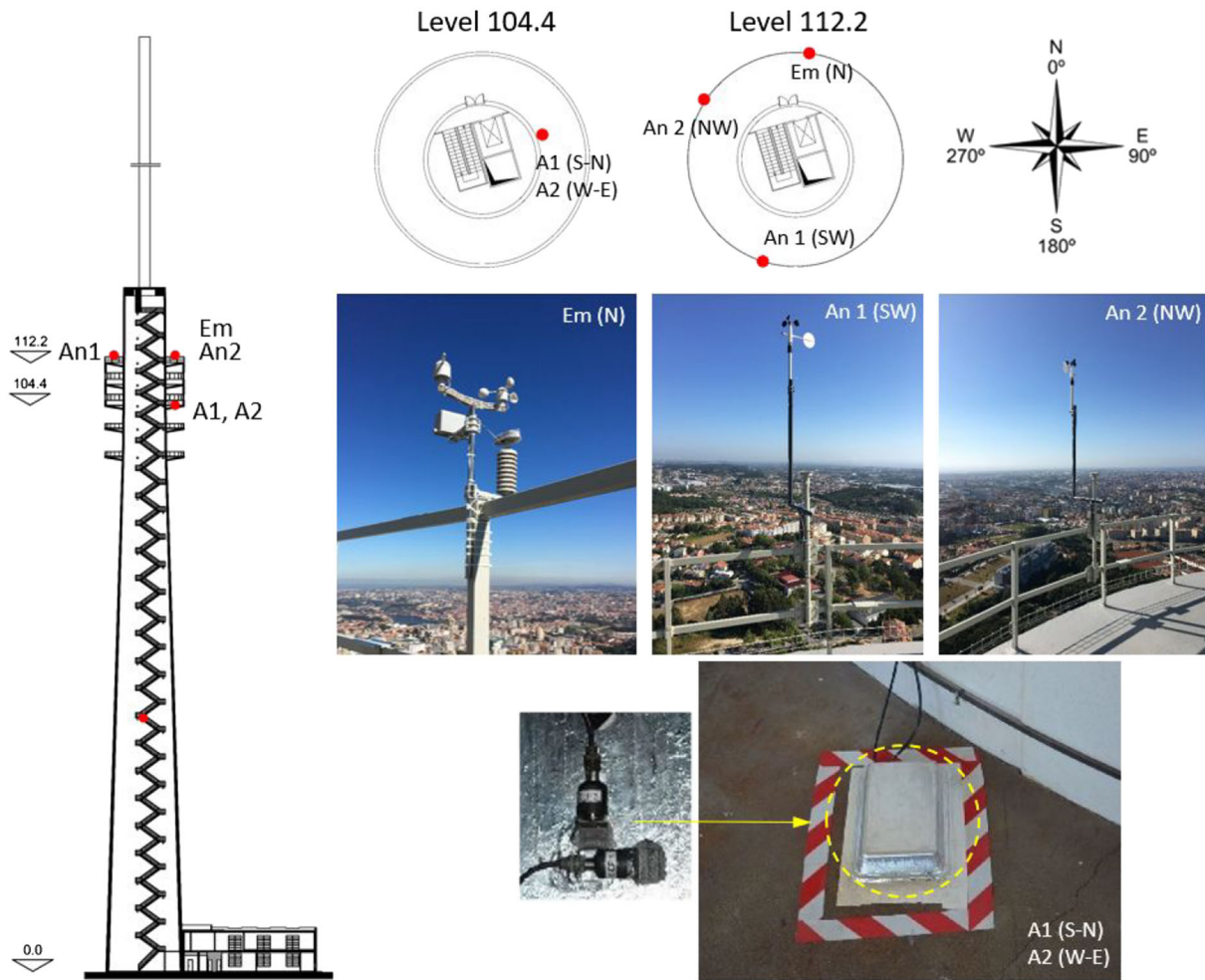


**FIGURE 2** Continuous monitoring system: Sensor positioning and measurement directions

Noncritical events are related to frequent events, which occur throughout the vast majority of the lifespan of the structure, and in which the maximum acceleration values ranged from 1.0 to 5.0 mg. As an example, Figures 3 and 4 show the typical acceleration records of two noncritical events (NC1 and NC2), over a period of 60 min, including the corresponding average and normalized auto spectra between DC and 5 Hz, obtained through Welch's method, and the direction and speed records of the wind with indication of its average values. The Welch's method considered equally spaced time-segments with a length equal to 4,096 points, a segment overlap of 50% and a Hamming time-window. The presented acceleration records are obtained through the vector sum of the signals of accelerometers A1 and A2.

Event NC1 depicts a typical occurrence of the daytime period, in which the wind predominantly comes from the North, with a very slight variation of direction and a speed varying from 25 to 50 km/h. The frequency content of the structure's dynamic response comprises an extended frequency range, with preponderance for the vibration modes related to the bending of the shaft and the metallic mast, with natural frequencies equal to 0.478 and 0.701 Hz, respectively.<sup>3,23</sup> These modes were identified based on the instrumentation of 13 measuring points during an ambient vibration test, 12 located in the concrete shaft and 1 located in the metallic mast.<sup>3</sup> The distinction between these two modes was possible by the modal information collected at the measuring point located on the metallic mast, which allowed to adequately scaling the movements of the mast in relation to the movements of the concrete shaft. Figure 5 shows the first two experimental modal configurations of the tower.

On the other hand, event NC2 depicts a typical occurrence of the nocturnal period, in which the wind comes predominantly from the South, typically with a negligible variation of direction and a speed varying from 10 to 30 km/h. The frequency content of the structure's dynamic response, as stated in the previous event, also occurs in an extended frequency range.

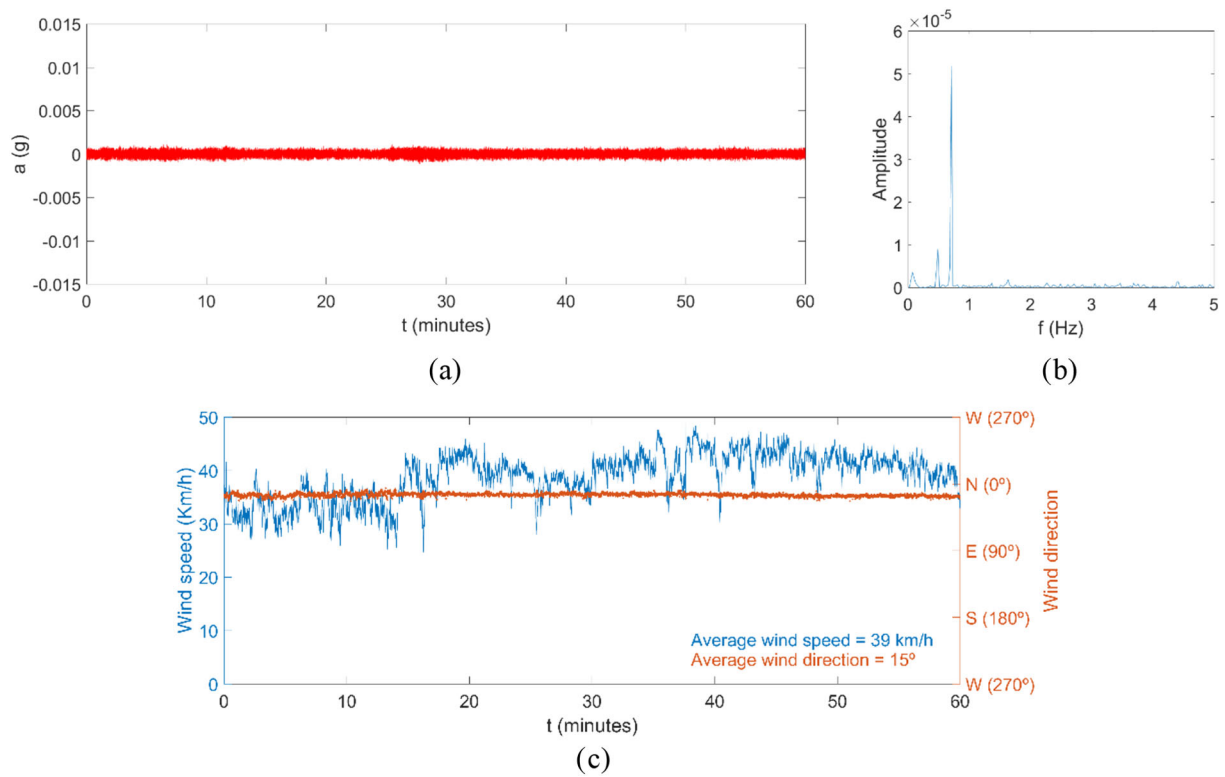


**FIGURE 3** Noncritical event NC1: (a) acceleration record, (b) average and normalized auto spectra of accelerations, and (c) records of wind speed and direction

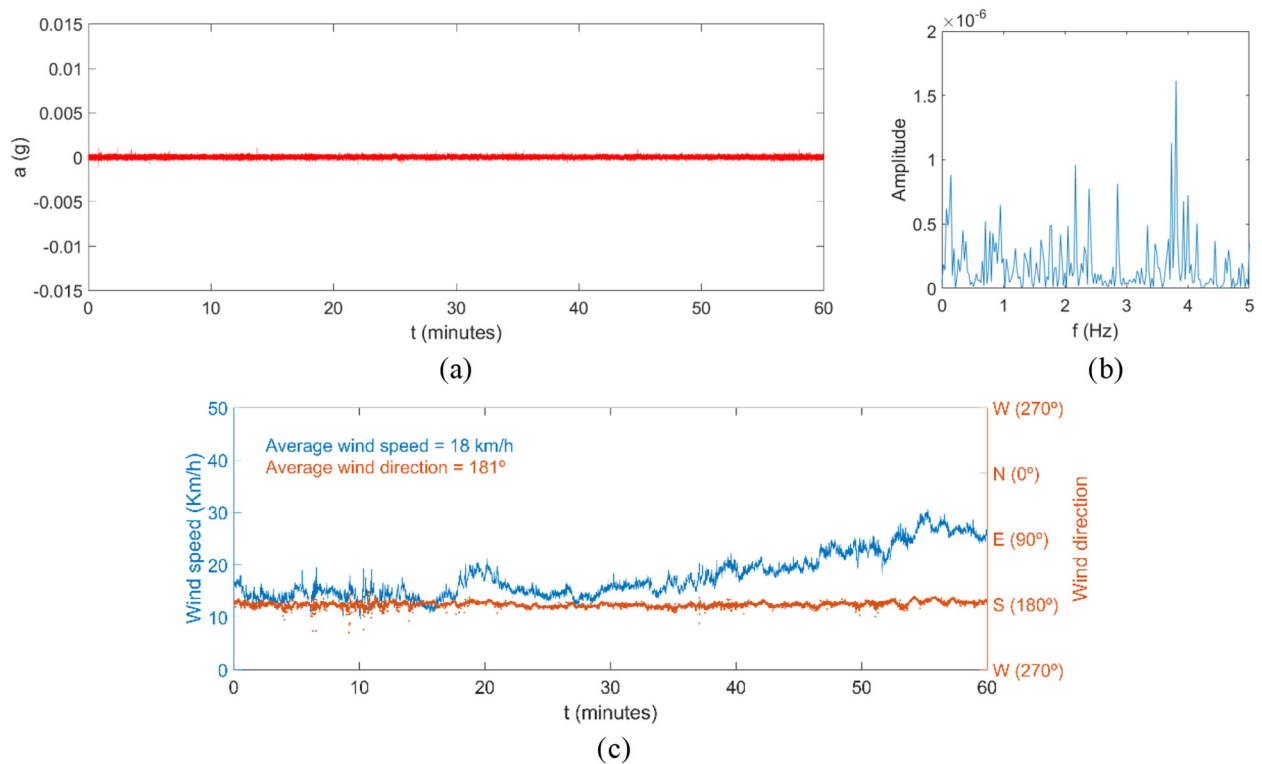
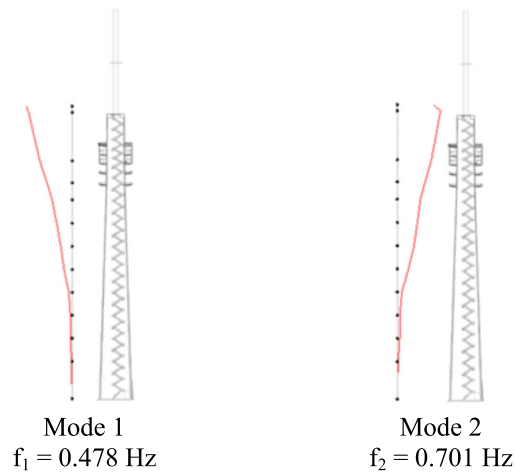


**FIGURE 4** Noncritical event NC2: (a) acceleration record, (b) average and normalized auto spectra of accelerations, and (c) records of wind speed and direction

FIGURE 5 Experimental modal configurations<sup>3</sup>



Critical events are related to lower-frequency occurrences associated with significant amplifications of the dynamic response, in which the maximum acceleration values ranged from 5.0 to 15.0 mg. This acceleration interval was defined as critical by the infrastructure manager. It is assumed that the serviceability and safety requirements will not be satisfied within the defined interval, in particular, staff comfort, normal equipment operation, and fatigue safety of the connections between the mast and the shaft, and of the mast itself.

As an example, Figures 6 and 7 present the typical acceleration records of two critical events (C1 and C2), over a period of 60 min, including the corresponding average and normalized auto spectra between DC and 5 Hz, obtained through Welch's method, and the direction and speed records of the wind with indication of its average values. Details of both acceleration records are also presented for a time window of 10 s. Once again, the presented acceleration records are obtained through the vector sum of the signals of accelerometers A1 and A2.

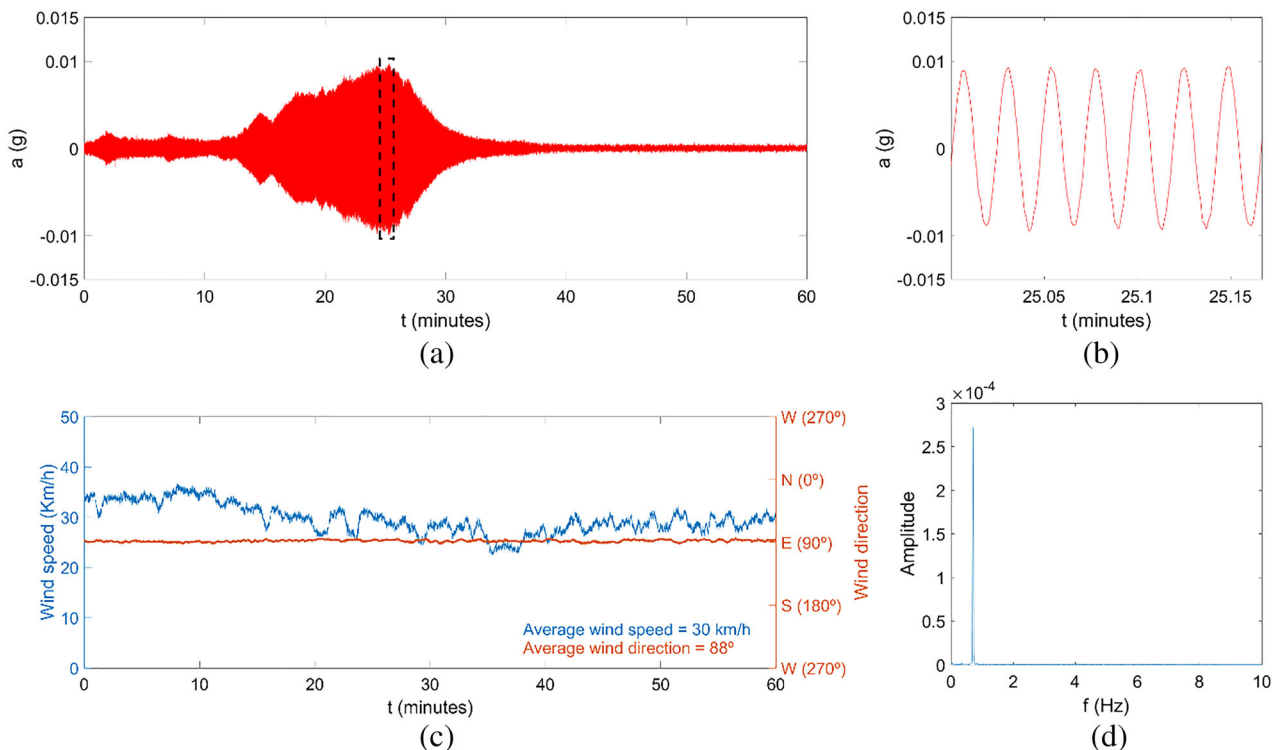
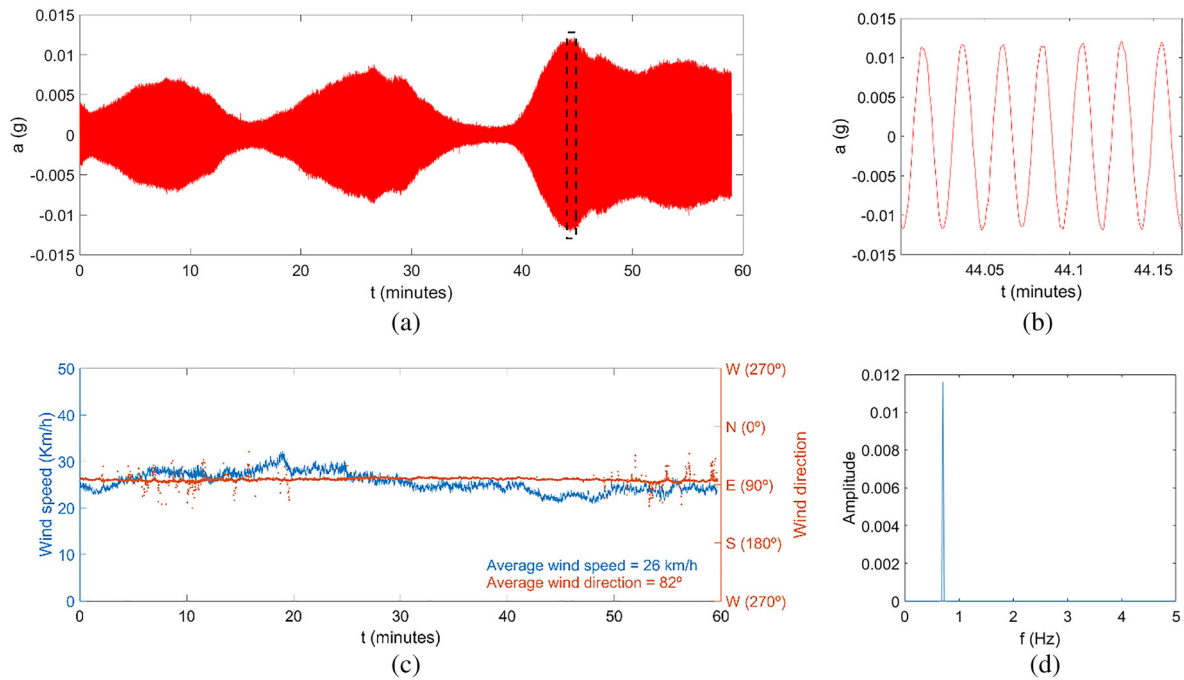


FIGURE 6 Critical event C1: (a) acceleration record, (b) detail of the acceleration record over 10 s, (c) records of wind speed and direction, (d) average and normalized auto spectra of accelerations



**FIGURE 7** Critical event C2: (a) acceleration record, (b) detail of the acceleration record over 10 s, (c) records of wind speed and direction, (d) average and normalized auto spectra of accelerations

The observation of both figures shows that the occurrence of critical events is usually associated with east winds, with practically no change in direction, and with constant speeds ranging between 20 and 35 km/h. The frequency content of the dynamic response of the structure presents the unique contribution of the vibration mode associated with the local bending of the metallic mast ( $f = 0.701$  Hz), which, due to structural compatibility, induces movements in the shaft. These events occurred due to a vortex-shedding phenomenon in the metallic mast which can be simply characterized based on a dimensionless parameter, the Strouhal number ( $S_t$ ), involving the characteristic values of wind speed ( $U$ ), cylinder diameter ( $D$ ), and vortex-shedding frequency ( $f$ ):

$$S_t = \frac{fD}{U} \quad (1)$$

Considering that  $f = 0.701$  Hz,  $D = 1.8$  m and that for cylinders of circular cross section the Strouhal number takes the value of 0.20, it results that the critical wind speed for the metallic mast is approximately equal to 6.31 m/s (22.7 km/h). This speed value fits within the range of velocities experimentally identified as being associated with the occurrence of critical events.<sup>3</sup>

Concerning the wind direction, east winds have practically no change of direction, and are typically characterized by quite predictable and constant speeds between 20 km/h and 35 km/h. In turn, for other wind directions, such as dominant north and south winds, the wind speeds are not always within the critical speed interval, besides presenting a larger speed variation. This variability is not favorable for the occurrence of vortex shedding phenomena.

More details on the automatic identification of critical events can also be found in reference.<sup>3</sup>

Sporadic events are associated with occasional situations in which the dynamic response of the structure under wind action is influenced by operational effects, such as lift movements, equipment in operation and the presence of technical staff during maintenance works. These events are characterized by acceleration peaks with maximum values that can reach 100 mg, largely exceeding the maximum values recorded in critical events.

As an example, Figure 8 presents the typical acceleration records of two sporadic events (S1 and S2), over a period of 60 min, including the corresponding average and normalized auto spectra between DC and 5 Hz obtained through Welch's method. Both records were filtered by a Chebyshev-type II low-pass digital filter with a cutoff frequency of 10 Hz, and were obtained through the vector sum of the signals of accelerometers A1 and A2.

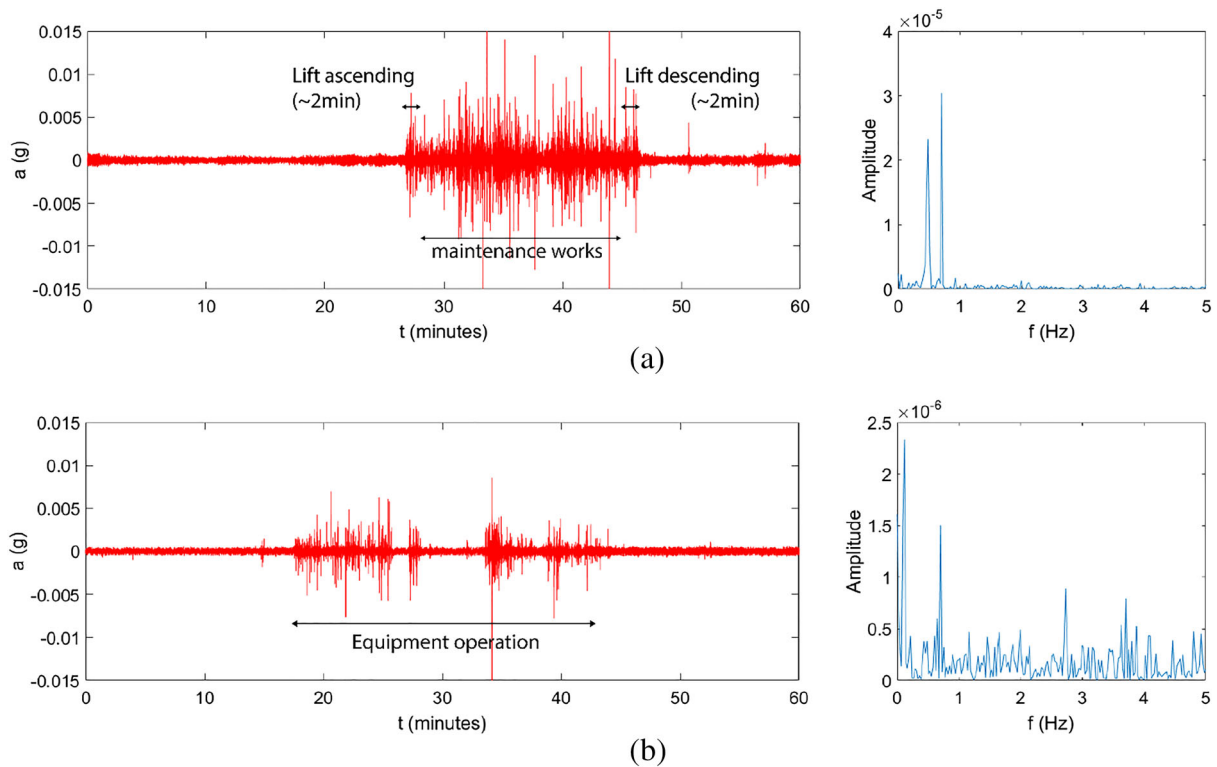


**FIGURE 8** Acceleration records of sporadic events and corresponding auto-spectra: (a) event S1, (b) event S2

The acceleration record shown in Figure 8a, just as other records of the same kind, includes an example of the influence of the lift movement (ascending and descending) and the presence of technical staff during maintenance works, which occur over a period of approximately 20 min. The analysis of the acceleration auto-spectra also shows that the operational effects mobilize a frequency range overlapped on the tower's natural frequencies, especially those associated with the bending of the shaft and the metallic tower, which prevents its removal by the application of digital filters.

In turn, the acceleration record shown in Figure 8b, just as other records of the same kind, includes an example of the influence of the operation of telecommunications equipment installed in the tower, lasting about 25 min. The analysis of the acceleration auto-spectra shows that operational effects seem to occur in a larger frequency range, which includes some of the structural vibration frequencies,<sup>3,23</sup> preventing once again, the application of digital filters for its removal.

## 4 | METHODOLOGIES TO AUTOMATICALLY REMOVE THE INFLUENCE OF OPERATIONAL EFFECTS

The development of robust methodologies that remove the influence of operational effects automatically and efficiently is crucial in a SHM system; otherwise, several events can be wrongly identified as critical. In order to accomplish this goal, two methodologies, one based on the PCA, and the other based on the crest factor (CF) and autoregressive (AR) models were developed and applied to the measured acceleration records.

### 4.1 | Methodology based on the PCA

#### 4.1.1 | Theoretical background

The PCA is a multivariate statistical method that consists of projecting the measured acceleration values, contained in a larger subspace, into a new set of Cartesian coordinates with reduced dimension, known as the principal subspace.<sup>5,9</sup>

Figure 9 summarizes the main steps of a PCA implementation using a SVD to find the principal components. The baseline correction of the acceleration records was based on a linear polynomial fitting.

Generally, the measured acceleration records are derived from the  $v$  sensors that were used; however, in the proposed methodology the records that were used resulted from the division, in equal parts, of the acceleration signal of only one sensor. Each part of the original record is called an event and includes  $n$  observations in correspondence with the measured acceleration values.

Thus, considering an acceleration time-series divided in  $v$  events, each one with  $n$  observations, the original data matrix ( $\mathbf{X}$ ) can be described as (Figure 9a):

$$\mathbf{X}_{(n \times v)} = [\mathbf{X}^1 \mathbf{X}^2 \mathbf{X}^3 \dots \mathbf{X}^v] = \begin{bmatrix} x_1^1 & x_1^2 & x_1^3 & \dots & x_1^v \\ x_2^1 & x_2^2 & x_2^3 & \dots & x_2^v \\ x_3^1 & x_3^2 & x_3^3 & \dots & x_3^v \\ \vdots & \vdots & \vdots & \ddots & \vdots \\ x_n^1 & x_n^2 & x_n^3 & \dots & x_n^v \end{bmatrix} \quad (2)$$

where  $x_j^i$  represents observation  $j$  of event  $i$ , while  $\mathbf{X}^i$  is the vector that includes the  $n$  observations associated with event  $i$ .

The PCA method uses a linear projection to convert the set of correlated observations referring to the Cartesian space of dimension  $v$  (Figure 9b), into a set of values of  $q$  uncorrelated variables called principal components (Figure 9d), with  $q < v$ , through the following expression:

$$\mathbf{Z}_{(n \times q)} = \mathbf{X}_{(n \times v)} \mathbf{U}_{(v \times q)} \quad (3)$$

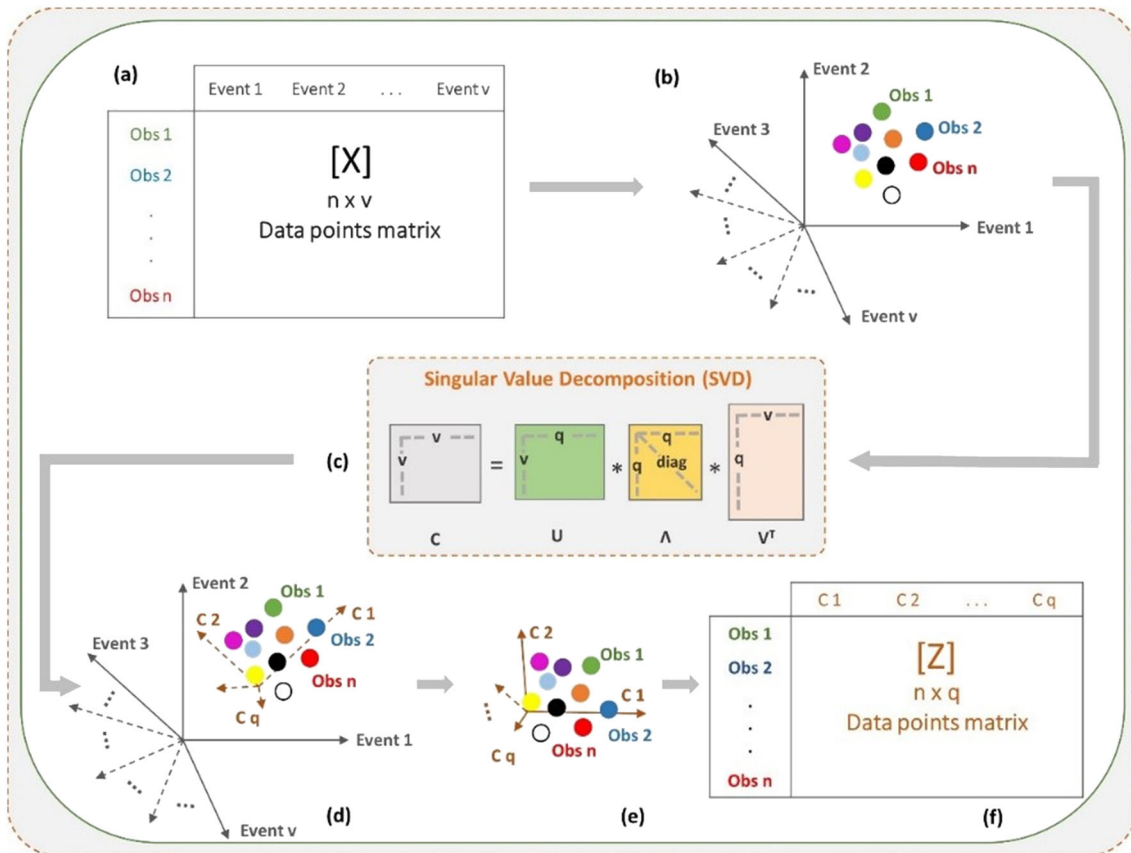


FIGURE 9 Flowchart of the principal component analysis implementation

where  $\mathbf{Z}_{(n \times q)}$  is the matrix with the transformed records,  $\mathbf{X}_{(n \times v)}$  is the matrix of the original events, and  $\mathbf{U}_{(v \times q)}$  is the transformation matrix (Figure 9e,f).

The transformation matrix  $\mathbf{U}$  can be obtained by the SVD of the covariance matrix  $\mathbf{C}_{(v \times v)}$ , by the following expression (Figure 9c):

$$\mathbf{C}_{(v \times v)} = \mathbf{U}_{(v \times q)} \mathbf{\Lambda}_{(q \times q)} \mathbf{V}_{(q \times v)}^T \quad (4)$$

where matrix  $\mathbf{C}$  is given by:

$$\mathbf{C}_{(v \times v)} = \begin{bmatrix} \text{var}(\mathbf{X}^1) & \text{cov}(\mathbf{X}^1 \mathbf{X}^2) & \cdots & \text{cov}(\mathbf{X}^1 \mathbf{X}^v) \\ \text{cov}(\mathbf{X}^2 \mathbf{X}^1) & \text{var}(\mathbf{X}^2) & \cdots & \text{cov}(\mathbf{X}^2 \mathbf{X}^v) \\ \vdots & \vdots & \ddots & \vdots \\ \text{cov}(\mathbf{X}^v \mathbf{X}^1) & \text{cov}(\mathbf{X}^v \mathbf{X}^2) & \cdots & \text{var}(\mathbf{X}^v) \end{bmatrix} \quad (5)$$

and  $\mathbf{U}$  is an orthonormal matrix, where the columns are the vectors that define the principal components,  $\mathbf{\Lambda}$  is a diagonal matrix with the principal components, and  $\mathbf{V}$  is the matrix containing the original space vectors.

If some of the principal components are removed, the inverse transformation can provide the corresponding re-projected data ( $\mathbf{X}'$ ):

$$\mathbf{X}'_{(n \times v)} = \mathbf{X}_{(n \times v)} \mathbf{U}_{(v \times q)} \mathbf{U}_{(q \times v)}^T \quad (6)$$

where matrix  $\mathbf{U}$  includes only the principal vectors of interest.

#### 4.1.2 | Criteria for the selection of the principal components

The automatic identification of the number of principal components to be removed is particularly relevant for the success of the PCA in eliminating the operational effects of the acceleration records.

Ballabio<sup>24</sup> proposes several selecting criteria for principal components that were designed to separate the principal components of the signal associated with the highest variances, that is, those that contribute most to their amplitude, from the principal components associated with the smallest variances and possibly associated with noise. Some of these criteria, namely the Average Eigenvalue Criterion (AEC),  $K_P$  and  $K_L$ , may also be used to separate the principal components associated with operational effects, typically with the largest signal amplitudes, from the principal components associated with wind effects and the lowest signal amplitudes.

The principal component selection criterion should, on the one hand, efficiently remove the operational effects from sporadic event acceleration records, and, on the other hand, not influence the critical and noncritical acceleration records. In addition, the selection criteria should be able to remove the different types of operating effects that occur in the tower.

The AEC indicator is derived from the solution of the singular value problem (Equation 4), in which the largest singular values (i.e., principal components) are associated with the largest variances. The AEC only accepts as significant the components with a singular value larger than the average singular value.<sup>24</sup>

Another strategy to select significant components is based on  $K$  correlation indicators ( $K_L$  and  $K_P$ ) which are multivariate indexes for quantifying the correlation content of the original data matrix (Expression 2).  $K_L$  estimates the maximum number of significant principal components under the assumption that the data is linearly correlated, while  $K_P$  computes the minimum number of significant components under the assumption that the information in the data decreases more steeply.<sup>24</sup> The linear ( $K_L$ ) and non-linear ( $K_P$ ) correlation indexes are derived as follows:

$$K_L = \text{int} [1 + (v-1)(1-K)] \quad (7)$$

$$K_P = \text{int} [v^{1-K}] \quad (8)$$

where  $\text{int}$  characterizes the nearest integer upper value,  $v$  is the number of events, which is equal to the number of correlated variables, and  $K$  is a constant that ranges between 0 (all variables are orthogonal) and 1 (all variables are perfectly correlated). The  $K$  value is automatically evaluated for each acceleration data matrix,  $\mathbf{X}$ , formed by  $v$  events, based on the application of the following expression<sup>24</sup>:

$$K = \sum_{i=1}^q \frac{\left| \frac{\mathbf{E}_i}{\sum_{j=1}^q \mathbf{E}_j} - \frac{1}{q} \right|}{2 \times \left( \sum_{j=1}^q \mathbf{E}_j - \frac{1}{q} \right)} \quad (9)$$

where  $q$  is the total number of principal components and  $\mathbf{E}_{(q \times 1)}$  is a column vector directly derived from the diagonal matrix  $\Lambda$ , which contains the  $q$  principal components values organized in descending order<sup>24</sup>:

$$\mathbf{E} = \frac{1}{(q-1)} \times \begin{bmatrix} \Lambda_{(1,1)}^2 \\ \Lambda_{(2,2)}^2 \\ \vdots \\ \Lambda_{(i,i)}^2 \\ \Lambda_{(q,q)}^2 \end{bmatrix} \quad (10)$$

### 4.1.3 | Proposed methodology

Figure 10 schematically presents the step-by-step instruction list of the methodology based on the PCA for the automatic removal of operational effects, originally developed by the authors using specific Matlab routines.<sup>25</sup>

### 4.1.4 | Influence of method parameters

In this section, the influence of some of the PCA method parameters is evaluated, namely, the criterion used for the selection of the principal components and the duration of the events, on the effectiveness of removing operational effects from the acceleration records.

#### *Influence of the principal components selection criteria*

Figure 11 illustrates the result of removing operational effects for the case of sporadic event S2, based on the indicators AEC,  $K_L$ , and  $K_P$ . Acceleration records are presented in the time interval [10–50] s to enhance the details in the area where the operational effects are most visible, with the original record in red and the post-PCA transformed record in blue. Additionally, in each figure, the number of principal components that have been removed from the transformed record, counted from the first principal component, is indicated. The duration of each event was considered equal to 60 s.

The observation of the figure shows that all criteria were efficient in removing operational effects, especially with regard to higher-amplitude acceleration peaks. The  $K_P$  criterion removed the smallest number of principal components, which conditioned its ability to eliminate some of the lower amplitude peaks derived from operational effects. Also, in the parts of the signal where the peaks were eliminated, it is visible that the base record, which is mainly associated with the effect of wind action, was slightly affected, as shown by the loss in signal amplitude. In turn, the AEC and

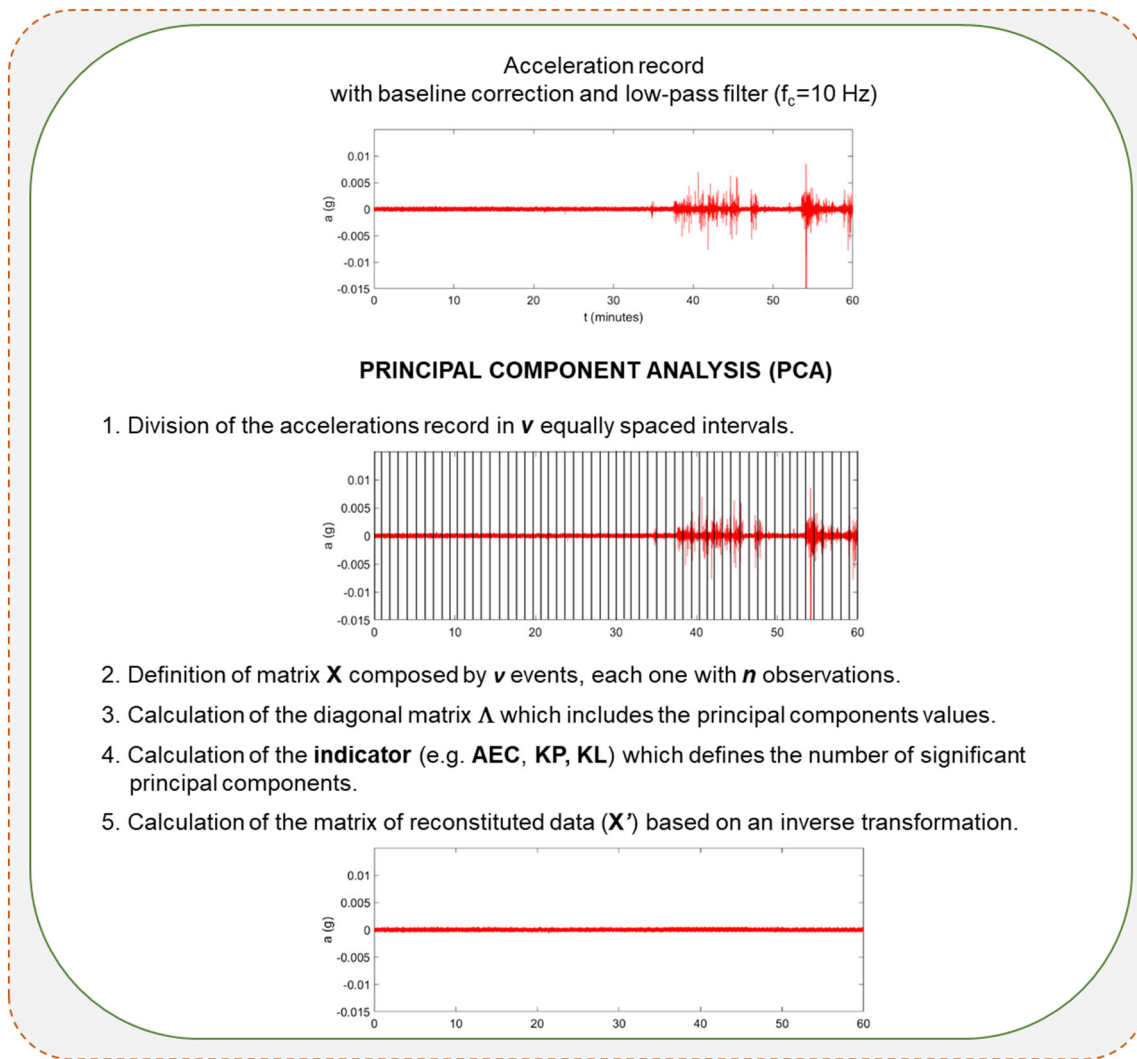


**FIGURE 10** Automatic removal of operational effects based on the principal component analysis method

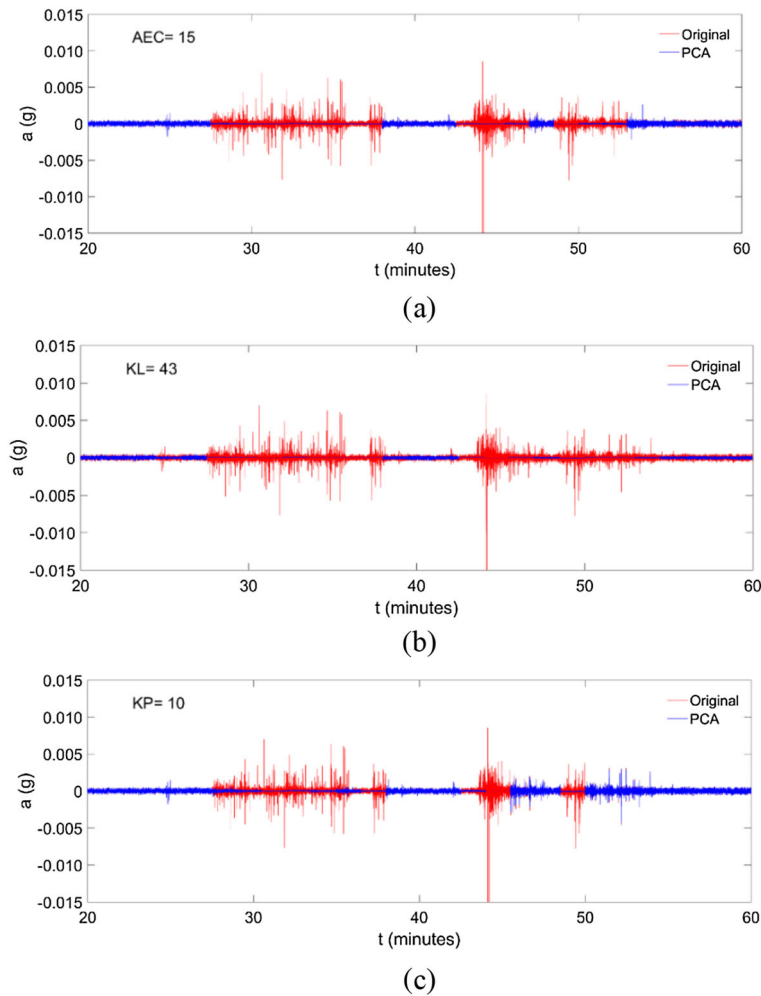
especially the  $K_L$  criteria proved to be more efficient in eliminating the operational effects and removed a larger number of principal components. In the case of the  $K_L$  criterion, all peaks associated with operational effects have been removed; however, larger extensions of the base record were affected with losses in the amplitude of the signal. The results obtained for sporadic event S2 are representative of what has been found for other sporadic events recorded in the tower.

Figure 12 presents the result of removing operational effects in the case of the critical event C2, based on the indicators AEC,  $K_L$ , and  $K_p$ . The purpose of this analysis is to evaluate the influence of the application of the principal component selection criteria in critical events, where the influence of operational effects is not visible. As in the previous figure, each plot shows the number of principal components that have been removed from the transformed record, counted from the first principal component. The duration of each event is equal to 60 s.

From the figure, it is possible to observe that, of the four criteria that were used, the  $K_p$  criterion is the only one that does not remove any principal components, and, therefore, does not affect the configuration of the critical event. The remaining criteria removed one principal component, in the case of the AEC, or two principal components, in the case of the  $K_L$ , significantly affecting the configuration of the corresponding records. The results obtained for the critical event C2 are representative of what was found for the remaining critical events measured in the tower.

Figure 13 presents the result of removing operational effects from the noncritical event NC2 based on the  $K_p$  indicator. A detail of the acceleration record is also presented for a time window of 10 s.

The results demonstrate that the PCA method slightly affected the signal amplitude since the first of the principal components was removed, but did not significantly affect the evaluation of the maximum signal amplitude. The results



**FIGURE 11** Principal component analysis-based removal of operational effects from the acceleration record of sporadic event S2 based on indicators: (a) AEC, (b)  $K_L$ , (c)  $K_P$

obtained for the noncritical event NC2 are representative of those found for the remaining noncritical events recorded in the tower, in which the first principal component was removed, or even, in many situations, in which no principal component was removed as desired.

Given the results shown in Figures 11 to 13, the  $K_P$  criterion was selected for the automatic removal of operational effects from the acceleration records.

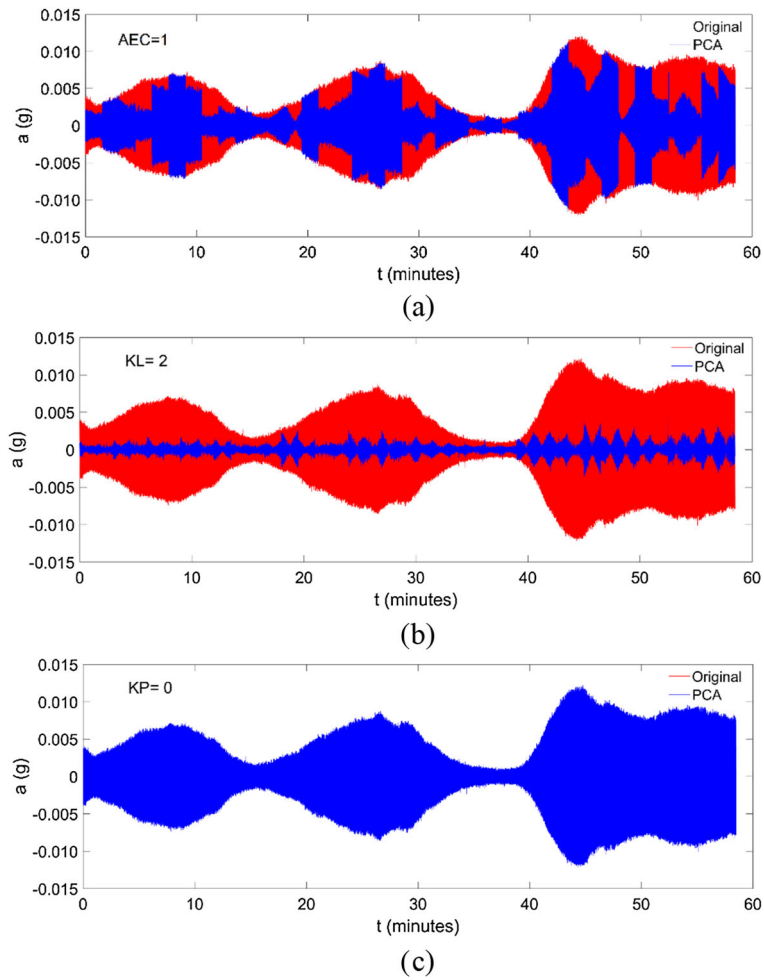
#### *Influence of event duration*

Figure 14 illustrates the result of removing operational effects from the sporadic event S2, based on different event durations, in this case 30, 60, and 90 s. The  $K_P$  was the principal component selection criterion.

The results show a tendency of the  $K_P$  criterion to improve its performance when a shorter duration of events is considered, especially between the 90 and 60 s records. However, it should be noted that the computational effort considering short duration events is very penalizing, as is the case of the duration of 30 s; therefore, a duration of 60 s was considered for the automatic removal of operational effects from the acceleration records.

### 4.1.5 | Application

Figure 15 presents the peak acceleration values, in mg, of the identified critical events based on the original data (Figure 15a) and the PCA-based method (Figure 15b) collected during a 3-month period, from September 1 to November 30, 2017.



**FIGURE 12** Principal component analysis-based removal of operational effects from the acceleration record of critical event C2 based on indicators: (a) AEC, (b)  $K_L$ , (c)  $K_P$

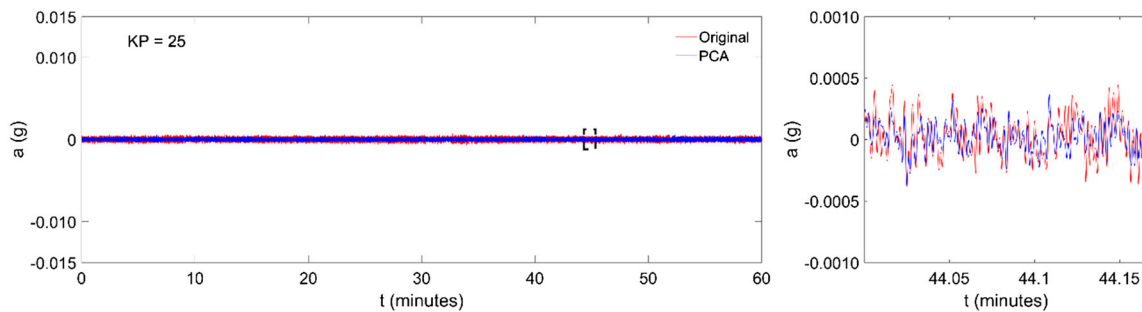


**FIGURE 13** Principal component analysis-based removal of operational effects from the acceleration record of noncritical event NC2 based on the indicator  $K_P$

The results show, especially in the original records, a very significant number of events with high peak accelerations, in some cases reaching values higher than 30 mg, which with the application of the PCA method were corrected to substantially lower values, since these were events influenced by operating conditions. These false-positives are related to events that could be classified as critical, given the original data, but in most cases, after applying the PCA method, they will be classified as noncritical events. In turn, for other identified events, the peak acceleration values of the original records and those after the PCA method are the same, demonstrating that these are the true critical events due to wind action.

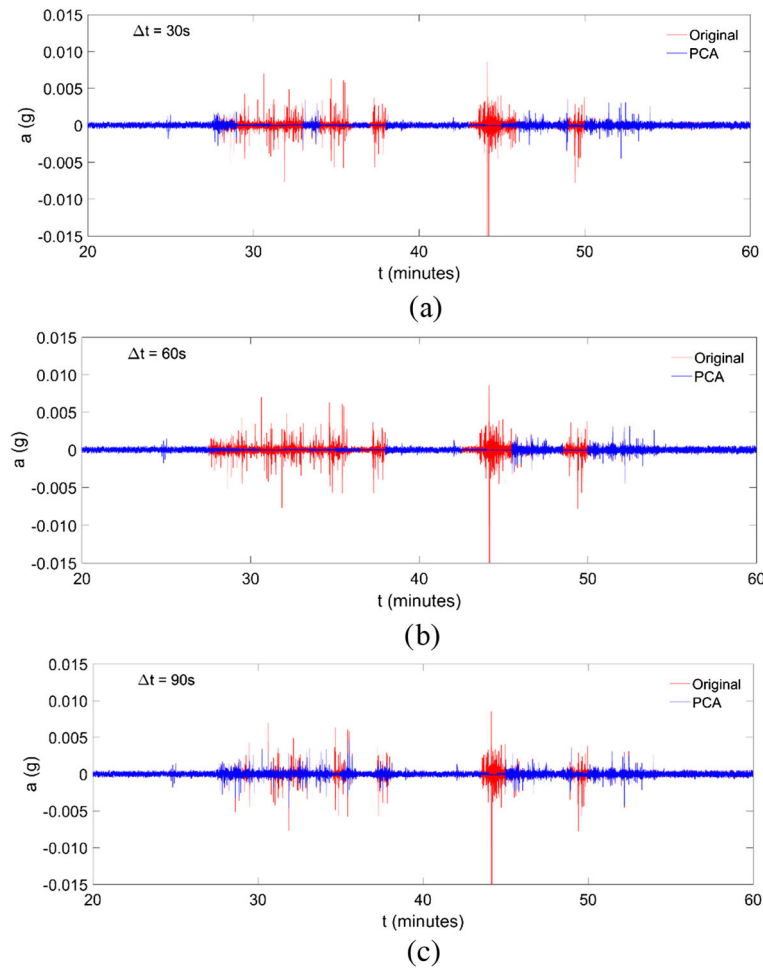


**FIGURE 14** Principal component analysis-based removal of operational effects from the acceleration record of sporadic event S2, based on different event durations: (a) 30 s, (b) 60 s, (c) 90 s

## 4.2 | Methodology based on the crest factor and autoregressive models

### 4.2.1 | Theoretical background

The second proposed methodology involves, first, the use of the CF to remove the parts of the acceleration records influenced by operational effects, and second, the application of an AR model to rebuild the parts removed from the signal. The baseline correction of the acceleration records was based on a linear polynomial fitting.

The CF is the ratio of the instantaneous peak amplitude of a time record and its RMS value (root mean square) according to the following expression:

$$CF_v = \frac{\max |\mathbf{X}^v|}{\mathbf{X}_{RMS}^v} \quad (11)$$

where  $\mathbf{X}^v$  is the vector that includes the  $n$  observations associated to event  $v$ , and  $\mathbf{X}_{RMS}^v$  is the corresponding RMS value given by:

$$\mathbf{X}_{RMS}^v = \sqrt{\frac{1}{n} \sum_{z=1}^n |x_z^v|^2} \quad (12)$$

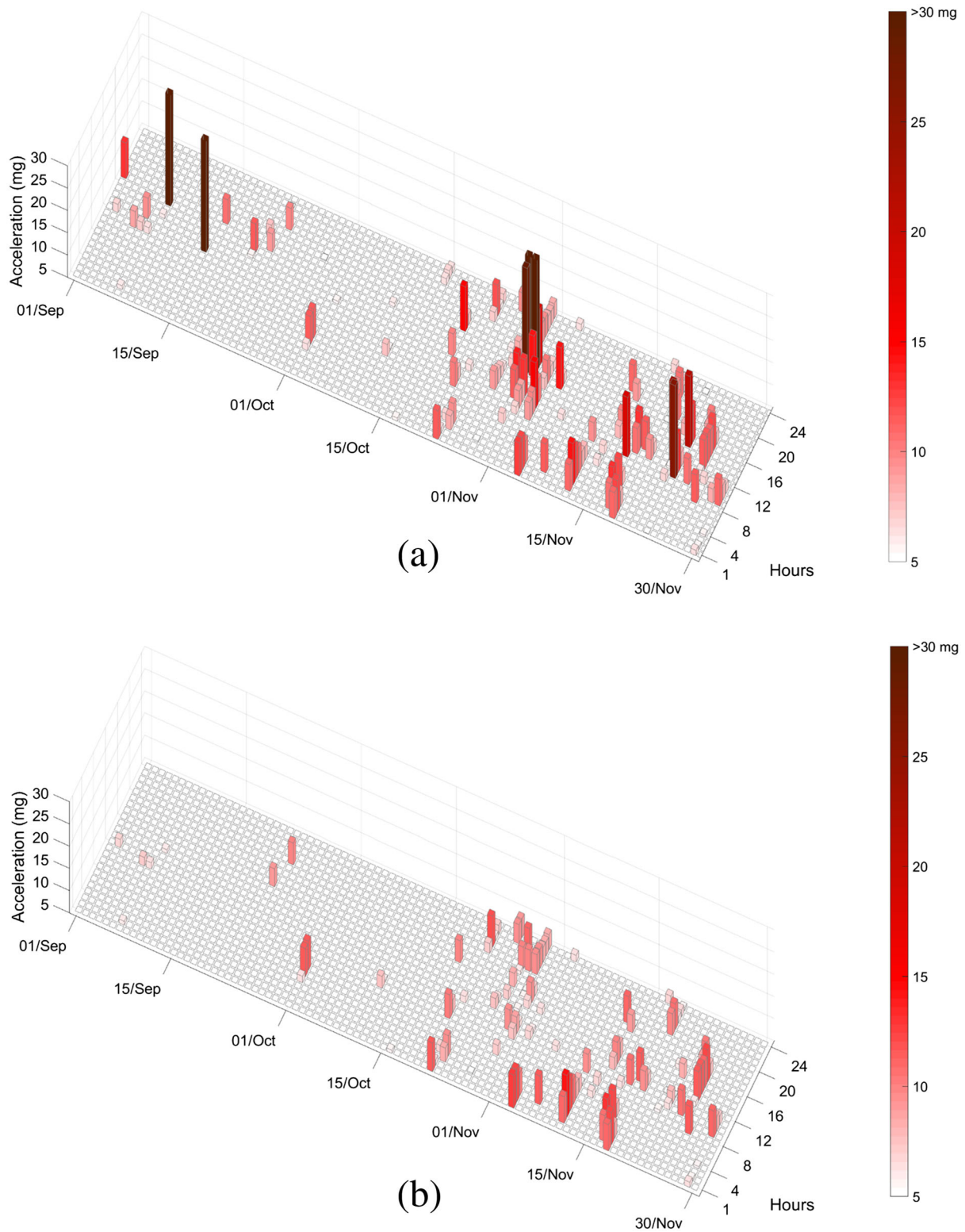


**FIGURE 15** Maximum acceleration values of critical events, in the range of 5 to >30 mg, between September 1 to November 30, 2017, based on (a) original data, (b) data processed by the principal component analysis-method

CF is a dimensionless quantity defined by a positive real number always equal or higher than 1.0. CF values close to 1.0 indicate similarity between instantaneous peaks in a time series. In the case of a pure sine wave, the CF value is equal to 1.41. Higher CF values indicate the presence of sporadic events in the time record.

Concerning the autoregressive model, generally designated as AR ( $p$ ), where  $p$  is the order of the model, it is a linear time series model defined by:

$$x_i = \sum_{j=1}^p x_{i-j} a_j \quad (13)$$

where the current value of the response,  $x_i$ , is defined as a linear combination of the  $p$  previous response values multiplied by the AR constant parameters  $a_j$ .

The appropriate order of the model can be determined by several methods, such as the Akaike's information criterion (AIC), the partial autocorrelation function (PAF), the SVD, the RMS, or the Bayesian information criterion (BIC).<sup>5,26</sup> In a matrix format, the AR model can be represented by:

$$\begin{bmatrix} x_{p+1} \\ x_{p+2} \\ \vdots \\ x_n \end{bmatrix} = \begin{bmatrix} x_1 & x_2 & \cdots & x_p \\ & x_2 & x_3 & \cdots & x_{p+1} \\ & & \vdots & \ddots & \vdots \\ x_{n-p} & x_{n-p+1} & \cdots & x_{n-1} & \end{bmatrix} \begin{bmatrix} a_p \\ a_{p-1} \\ \vdots \\ a_1 \end{bmatrix} \quad (14)$$

Typical time series lead to an overdetermined set of equations that must be solved to obtain estimates of the AR coefficients. There are many methods that can be used to solve the coefficients, including the Yule-Walker approach or the least squares method.<sup>5</sup>

## 4.2.2 | Proposed methodology

Figure 16 is a schematic representation of the step-by-step instruction list of the methodology based on the crest factor and autoregressive models for the automatic removal of operational effects, originally developed by the authors using specific Matlab routines.<sup>25</sup>

In the present study, the acceleration hourly records were divided into 60 intervals, each lasting 60 s. The threshold associated with the CF was considered equal to 5.0. This value was defined based on an extensive preliminary analysis of 24,480 subrecords, each one with 1 min duration, in the period between October 15 and 31, 2017. The results demonstrated that the CF values are typically between 1.47 and 3.0, for critical events, between 3.0 and 5.0, for noncritical events, and higher than 5.0 in case of sporadic events or isolated peak events related to electrical noise interferences.

The order of the AR model was 25, applying the SVD criterion according to the details of reference,<sup>3</sup> and the AR coefficients were calculated based on the acceleration records immediately before the removed parts. Thus, the reconstituted signals are obtained from previous experimentally measured time-series which already contains the usual disturbances that typically contaminates this type of signals.

Figure 17 illustrates the application of the AR model in reconstructing the eliminated parts of measured acceleration signals. The original signal (in red) is deliberately truncated after the first minute and the AR model is used to estimate the truncated part (in black) over a period of 1 min (Figure 17a) and 20 min (Figure 17b). The 20 min prediction, corresponds, approximately, to the longest duration of the sporadic event registered in Section 3.2. The comparison between the original and the estimated time-series proves the efficiency of the AR model in reconstructing the eliminated parts of the acceleration signals. Both, original and estimated time series, present approximately zero mean values and standard deviations (in mg) equal to 0.2364 and 0.2400, for the 1 min prediction, and 0.2437 and 0.2399, for the 20 min prediction. The largest percentual difference between the standard deviation values of the original and reconstructed time series is equal to 1.57%.

## 4.2.3 | Application

Figures 18 and 19 illustrate the result of removing operational effects from sporadic events S1 and S2. The acceleration records of events S1 and S2 are presented in the time intervals [20–60] and [10–50] s, respectively, to enhance the

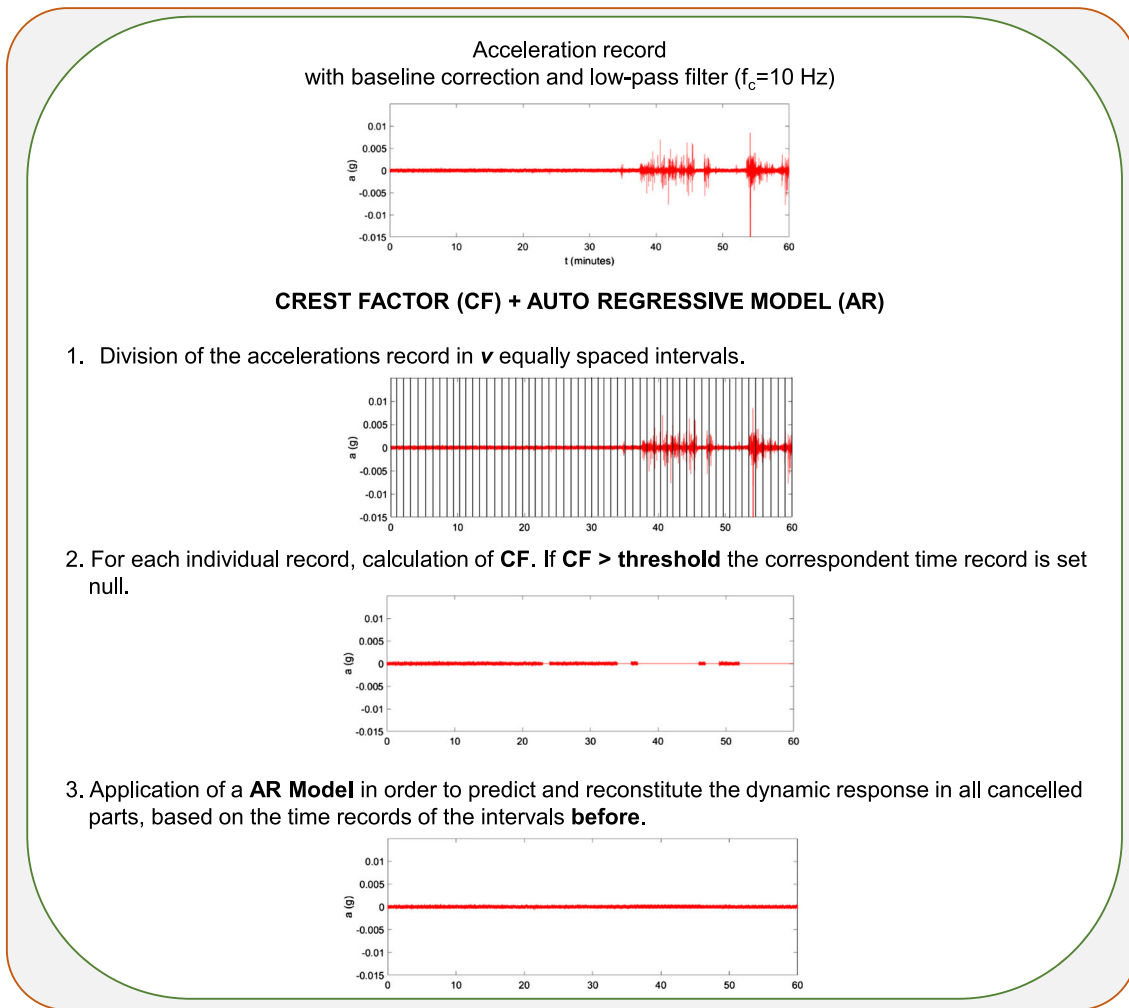


**FIGURE 16** Automatic removal of operational effects based on the crest factor and the autoregressive model

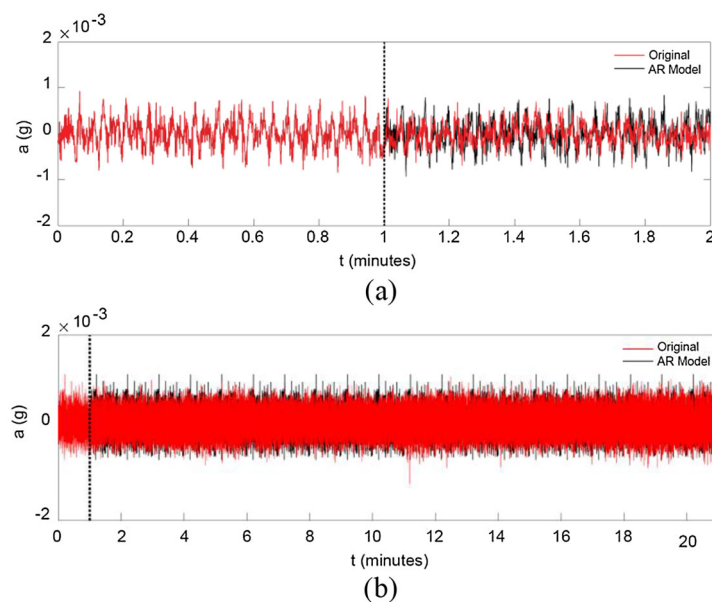


**FIGURE 17** Comparison between the original signal and the signal estimated using an autoregressive model: (a) 1 min prediction, (b) 20 min prediction

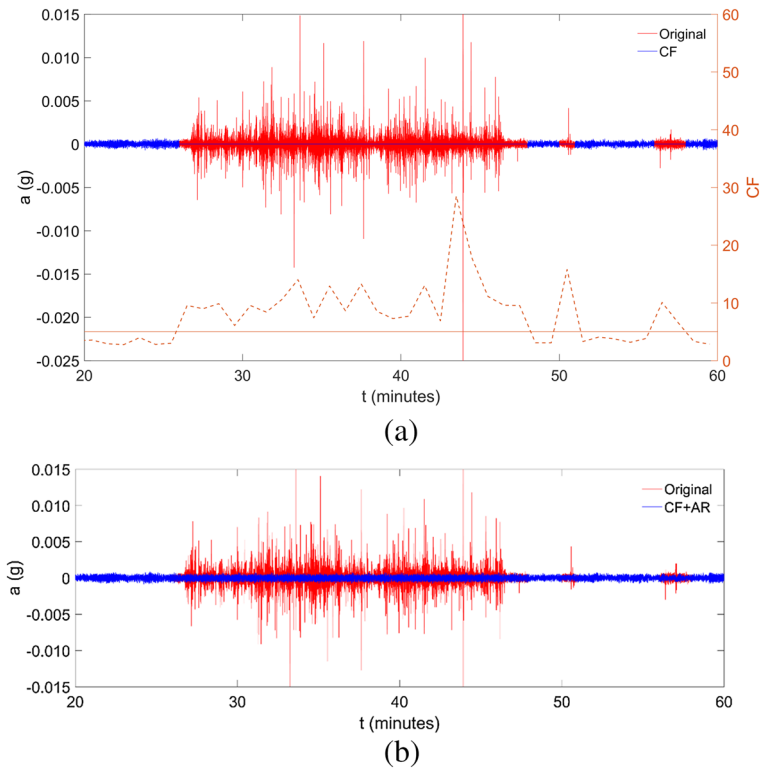


**FIGURE 18** Methodology for removing operational effects based on the crest factor (CF) and the autoregressive (AR) model for the acceleration record of sporadic event S1: (a) step 2 (CF only), (b) step 3 (CF and AR)

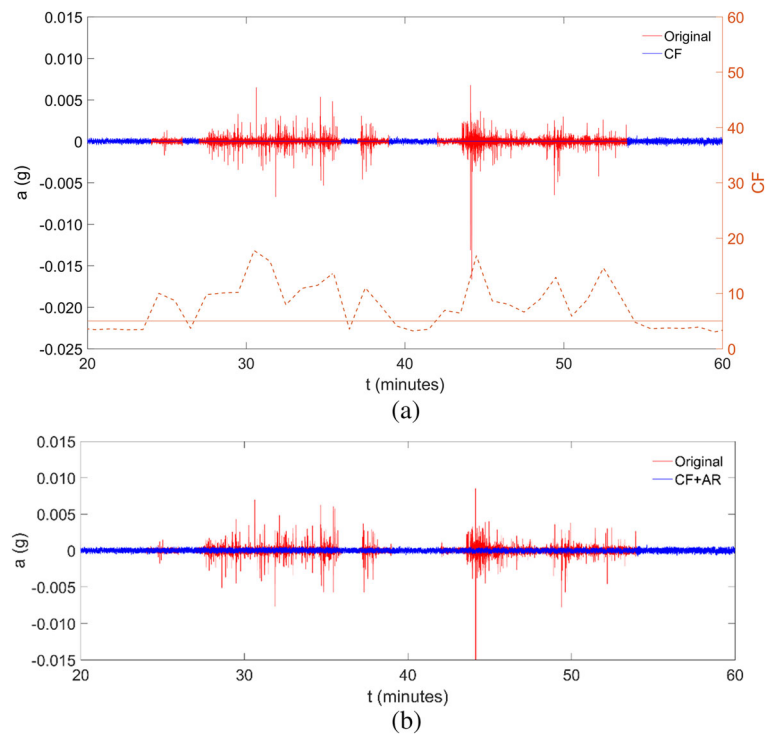


**FIGURE 19** Methodology for removing operational effects based on the crest factor (CF) and the autoregressive (AR) model for the acceleration record of sporadic event S2: (a) step 2 (CF only), (b) step 3 (CF and AR)

details in the zone where the operational effects are most visible, with the original record being represented in red and the transformed records represented in blue. In the case of transformed records, phased results are presented, namely from step 2 (after applying the CF, Figures 18a and 19a) and from steps 2 and 3 (after applying the CF and the AR model, Figures 18b and 19b), following the indications of Figure 16. In case of Figures 18a and 19a the CF values for each subrecord, as well as the threshold value equal to 5.0, are also presented.

In both events, the application of the CF proved to be extremely efficient in removing the parts of the records that are influenced by operational effects, as can be seen by the elimination of all the highest amplitude peaks, and almost all the smaller amplitude peaks, with occasional exceptions that are almost imperceptible.

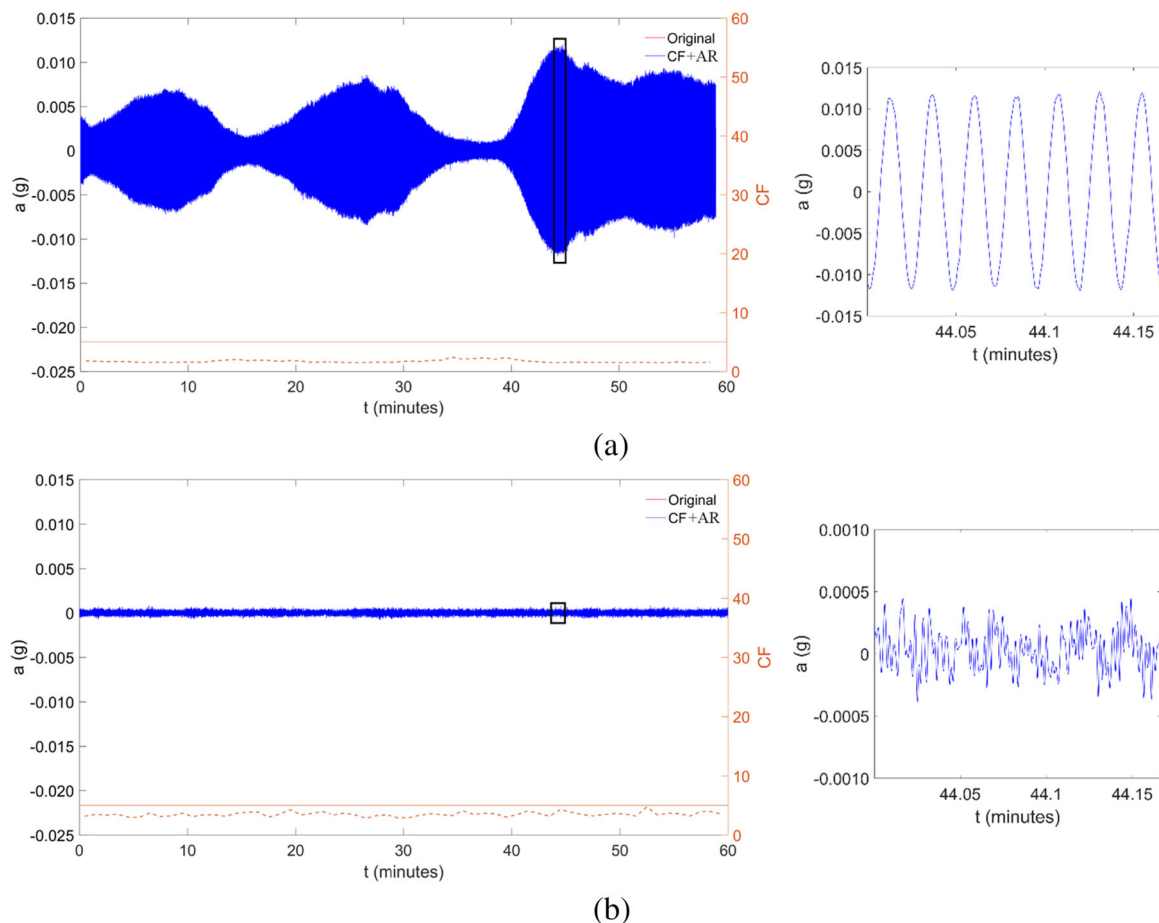
In addition, the AR model demonstrated a high robustness in the reconstruction of the parts of the acceleration records affected by operational effects. Furthermore, these parts of the records were not affected with losses in the amplitude of the signal. The results obtained for sporadic events S1 and S2 are representative of those found for other sporadic events recorded in the tower.

Figure 20 presents the result of removing operational effects in the case of the critical event C2 (Figure 20a) and the noncritical event NC2 (Figure 20b). Additionally, the CF values for each sub-record, as well as the threshold value equal to 5.0, are also presented. Details of the acceleration records are also presented for a time window of 10 s.

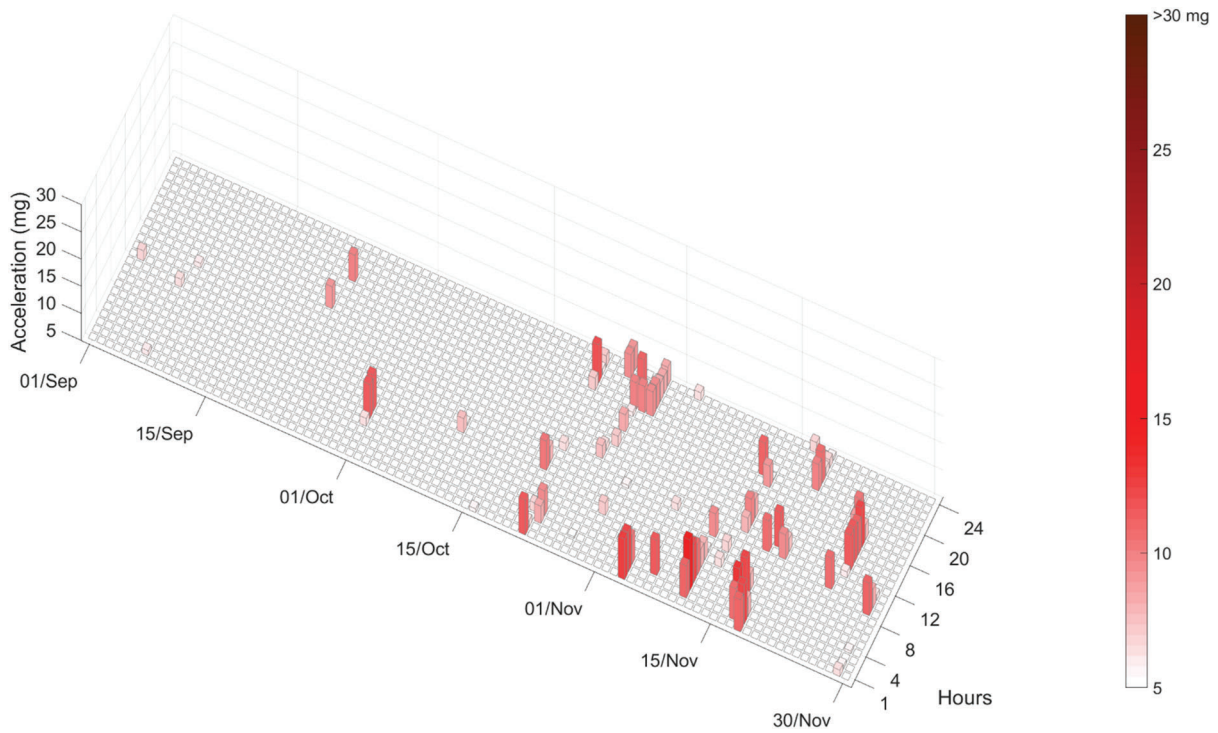
In both cases, once again, the results demonstrated the robustness of the methodology based on the CF and the AR model that keeps the original acceleration records unchanged.

Figure 21 presents the peak acceleration values, in mg, of the identified critical events for a 3-month period, from September 1 to November 30, 2017, obtained from the application of the CF and the AR model.

When comparing the obtained results with the maximum acceleration values of the original records (Figure 15a), it is possible to observe the extreme efficiency of the CF and AR method in eliminating a significant set of events associated with operational effects, most of them with high peak acceleration levels. Compared to the PCA method, the



**FIGURE 20** Methodology for removing operational effects based on the crest factor (CF) and the autoregressive (AR) model for the acceleration records of events: (a) critical C2, (b) noncritical NC2



**FIGURE 21** Maximum acceleration values of critical events, in the range of 5 mg to >30 mg, between September 1 and November 30, 2017, based on data processed by the crest factor and autoregressive method

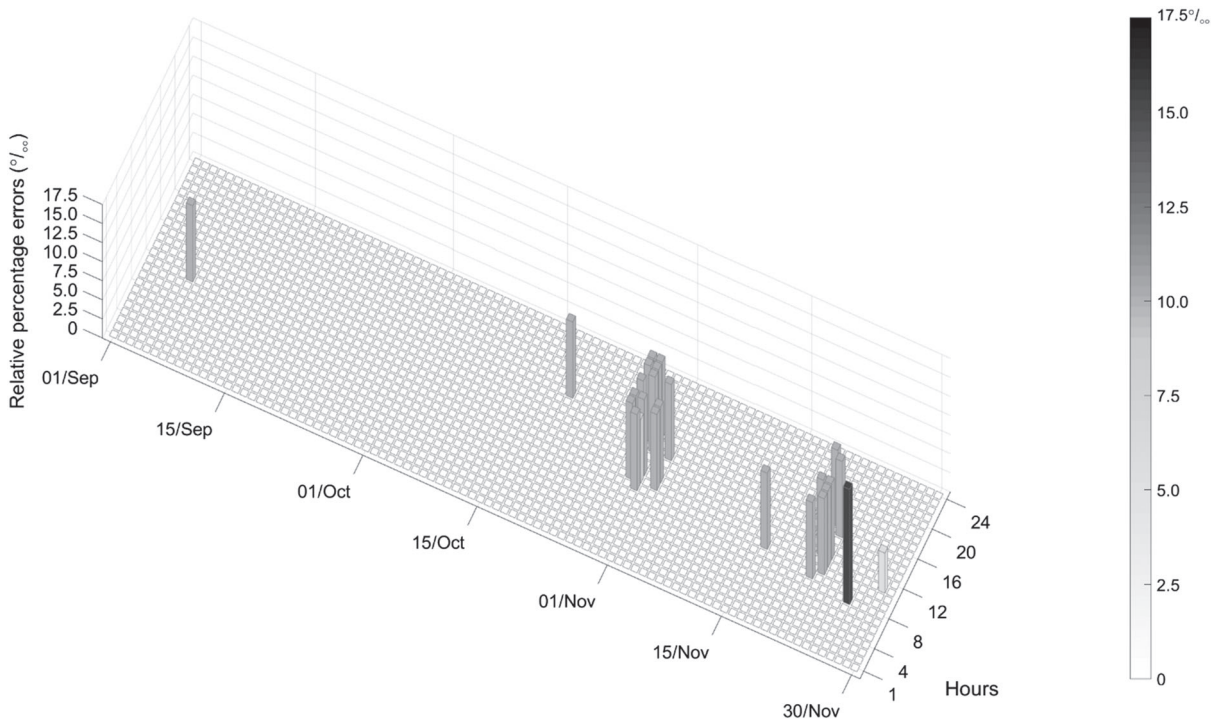


**FIGURE 22** Relative ppt errors of estimated maximum acceleration values based on the principal component analysis method and the crest factor and autoregressive method

method now proposed was able to identify a greater number of false-positive situations, which proves its greater stability and robustness.

In the period under analysis, 113 critical events were identified and the maximum recorded acceleration was 14.4 mg.

### 4.3 | Comparative analysis

Figure 22 shows the relative errors of the maximum acceleration values estimated based on the PCA method and the CF and AR method, in parts per thousand (ppt), and taking as reference the values of the CF and AR method. A relative error of 0 ppt means that the estimate of the maximum acceleration values of both methods is identical, while a positive relative error demonstrates that the estimate provided by the PCA method is greater than the one provided by the CF and AR method.

The results show, once again, the greater robustness and efficiency of the CF and AR method in eliminating the operational effects, as attested by the number of situations (25 in total) in which the PCA method was unable to adequately correct the maximum values of the acceleration records of sporadic events.

Another relevant aspect concerns the calculation time required to remove the operational effects from the 3 months acceleration records. In the case of the PCA method, the information processing was performed in about 14 h, while in the CF and AR method it was performed in approximately 1 h 30 min.

## 5 | CONCLUSIONS

The present study described the development and application of statistical methodologies to remove the operational effects from the dynamic responses of the Monte da Virgem telecommunications tower.

The characterization of the dynamic responses of the structure, over a period of 3 months, was based on a continuous monitoring system.

The analysis of the results allowed identifying several critical events, associated with significant amplifications of the dynamic response, with peak values between 5 and 15 mg, and typically occurring for east winds with speeds ranging between 20 and 35 km/h. These events occurred due to a vortex-shedding phenomenon on the metallic mast that mobilized local movements of the mast, which, indirectly and due to structural compatibility, induced movements on the shaft. Additionally, a significant number of sporadic events, associated with operational effects due to the movements of the lift, technical staff and equipment, were identified. These specific events were characterized by acceleration peaks with maximum values that reached 100 mg, largely exceeding the maximum values recorded for critical events.

The automatic identification of critical events is extremely important for the evaluation of the safety and serviceability conditions of the tower. Typically, this identification is performed based on the evaluation of the extreme acceleration values, and, therefore, it is necessary to remove the operational effects from the records beforehand.

The removal of the operational effects from the accelerations records was performed using two distinct methodologies, one based on the PCA and the other based on the CF, and AR models.

The success of the PCA is strongly related to the adequate selection of an automatic criterion for the removal of the principal components related to operational conditions. The  $K_p$  correlation criterion demonstrated a better performance than the AEC and the  $K_L$  criteria, mainly because it was able to remove almost every operational effect from the sporadic events, without influencing, or with negligible influence, on critical and non-critical events, respectively.

The second proposed methodology involves, first, the use of the CF to remove the parts of the acceleration records influenced by operational effects, and second, the application of an AR model to rebuild the removed parts of the signal. This approach showed efficiency and robustness in eliminating the acceleration peaks due to operational effects, as stated by the smaller number of false-positive occurrences in the identification of critical events, besides having a better computational performance, as revealed by the considerably less computational time required in comparison to the PCA method. The application of the CF and AR method precisely estimated, for the 3 months' period under analysis, 113 critical events and a maximum acceleration of 14.4 mg.

In terms of overall performance, the PCA method was not able to adequately remove the operational effects from 25 of the sporadic events, which were wrongly classified as critical events. However, the CF and AR method was able to

successfully remove the operational effects from these events, which were later classified as non-critical. The use of the original acceleration records, without any pre-processing for the removal of operational effects, will clearly overestimate the number of critical events.

In future works, the authors intend to modify the PCA method in order to upgrade its ability in identifying and correcting sporadic events in telecommunications towers, and explore new methods based on machine learning approaches.

## ACKNOWLEDGMENTS

The authors express their gratitude to Altice, particularly to Engineer Jorge Garcia, for all the information provided about the Monte da Virgem telecommunications tower, and for all the support and facility access provided during the continuous monitoring of the tower. The authors would like to acknowledge the support of the Base Funding - UIDB/04708/2020 of the CONSTRUCT - Instituto de I&D em Estruturas e Construções - funded by Portuguese national funds through the FCT/MCTES (PIDDAC).

## ORCID

Diogo Ribeiro  <https://orcid.org/0000-0001-8624-9904>

Jorge Leite  <https://orcid.org/0000-0002-5581-0356>

Andreia Meixedo  <https://orcid.org/0000-0001-8327-1452>

Nuno Pinto  <https://orcid.org/0000-0001-8353-8663>

Rui Calçada  <https://orcid.org/0000-0002-2375-7685>

Michael Todd  <https://orcid.org/0000-0002-4492-5887>

## REFERENCES

1. Beirou B, Osterrieder P. Dynamic investigations of TV towers. *Structural engineering. Mechanics and Computation*. 2001;1:629-636.
2. Qiusheng L, Yinghou H, Kang Z, Xuliang H, Yuncheng H, Zhenru S. Structural health monitoring for a 600 m high skyscraper. *Structural Design of Tall and Special Buildings*. 2018;27(12):e1490.
3. Ribeiro D, Leite J, Pinto N, Calçada R. Continuous monitoring of the dynamic behaviour of a high-rise telecommunications tower. *Structural Design of Tall and Special Buildings*. 2019;28(11):e1621.
4. Guo Y, Kareem A, Ni Y, Liao W. Performance evaluation of Canton tower under winds based on full-scale data. *Journal of Wind Engineering and Industrial Aerodynamics*. 2012;104-106:116-128.
5. Farrar C., Worden K. (2013). *Structural health monitoring—A machine learning approach*, 1st edition, John Wiley & Sons Ltd, UK.
6. Moughty J, Casas J. A state of the art review of modal-based damage detection in bridges: development, challenges, and solutions. *Applied Sciences*. 2017;7(5):510-534.
7. Magalhães F, Cunha A, Caetano E. Vibration based structural health monitoring of an arch bridge: From automated OMA to damage detection. *Mechanical Systems and Signal Processing*. 2012;28:212-228.
8. Comanducci G, Ubertini F, Materazzi A. Structural health monitoring of suspension bridges with features affected by changing wind speed. *Journal of Wind Engineering and Industrial Aerodynamics*. 2015;141:12-26.
9. Santos J, Crémone C, Orcesi A, Silveira P. Multivariate statistical analysis for early damage detection. *Engineering Structures*. 2013;56:273-285.
10. Tjirkallis A, Kyprianou A. Damage detection under varying environmental and operational conditions using wavelet transform modulus maxima decay lines similarity. *Mechanical Systems and Signal Processing*. 2016;66-67(66-67):282-297.
11. Tomé E, Pimentel M, Figueiras J. Online early damage detection and localization using multivariate data analysis: Application to a cable stayed bridge. *Structural Control and Health Monitoring*. 2019;26(11):e2434.
12. Figueiredo E, Todd M, Farrar C, Flynn E. Autoregressive modeling with state-space embedding vectors for damage detection under operational variability. *International Journal of Engineering Science*. 2010;48(10):822-834.
13. Cury A, Crémone C, Dumoulin J. Long-term monitoring of a PSC box girder bridge: Operational modal analysis, data normalization and structural modification assessment. *Mechanical Systems and Signal Processing*. 2012;33:13-37.
14. Cross E, Koo K, Brownjohn J, Worden K. Long-term monitoring and data analysis of the Tamar bridge. *Mechanical Systems and Signal Processing*. 2011;35(1-2):16-34.
15. Zou H, Ni Y, Ko J. Structural damage alarming using auto-associative neural network technique: exploration of environment-tolerant capacity and setup of alarming threshold. *Mechanical Systems and Signal Processing*. 2011;25(5):1508-1526.
16. Li H, Li S, Ou J, Li H. Modal identification of bridges under varying environmental conditions: Temperature and wind effects. *Structural Control and Health Monitoring*. 2010;17(5):495-512.
17. Hsu T, Loh C. Damage detection accommodating nonlinear environmental effects by nonlinear principal component analysis. *Structural Control and Health Monitoring*. 2010;17(3):338-354.
18. Santos J, Cremona C, Calado L, Silveira P, Orcesi A. On-line unsupervised detection of early damage. *Structural Control and Health Monitoring*. 2016;23(7):1047-1069.

19. Deraemaeker A, Reynders E, de Roeck G, Kullaa J. Vibration-based structural health monitoring using output-only measurements under changing environment. *Mechanical Systems and Signal Processing*. 2008;22(1):34-56.
20. Hu W, Thöns S, Rohrmann R, Said S, Rucker W. Vibration-based structural health monitoring of a wind turbine system part II: Environmental/operational effects on dynamic properties. *Engineering Structures*. 2015;89:273-290.
21. Nie Z, Guo E, Li J, Hao H, Ma H, Jiang H. Bridge condition monitoring using fixed moving principal component analysis. *Structural Control and Health Monitoring*. 2020;27(6):e2535.
22. Datteo A, Lucà F, Busca G. Statistical pattern recognition approach for long-time monitoring of the G. Meazza stadium by means of AR models and PCA. *Engineering Structures*. 2017;153:317-333.
23. Ribeiro D., Leite J., de Pauli R., Alves V., Costa B., Calçada R. (2017). Calibration of the numerical model of a telecommunications tower based on genetic algorithms. *Genetic Algorithms: Advances in Research and Applications*, Chapter 3, Nova Publishers, USA.
24. Ballabio D. A MATLAB toolbox for principal component analysis and unsupervised exploration of data structure. *Chemometrics and Intelligent Laboratory Systems, 149 Part B*. 2015;1-9.
25. Mathworks. (2001). MATLAB—Getting started guide. Natick, USA.
26. Figueiredo E, Park G, Farrar C, Worden K, Figueiras J. Machine learning algorithms for damage detection under operational and environmental variability. *Structural Health Monitoring*. 2011;10(6):559-572.

**How to cite this article:** Ribeiro D, Leite J, Meixedo A, Pinto N, Calçada R, Todd M. Statistical methodologies for removing the operational effects from the dynamic responses of a high-rise telecommunications tower. *Struct Control Health Monit*. 2021;e2700. <https://doi.org/10.1002/stc.2700>